

*Electronic Supplementary Information (ESI)*

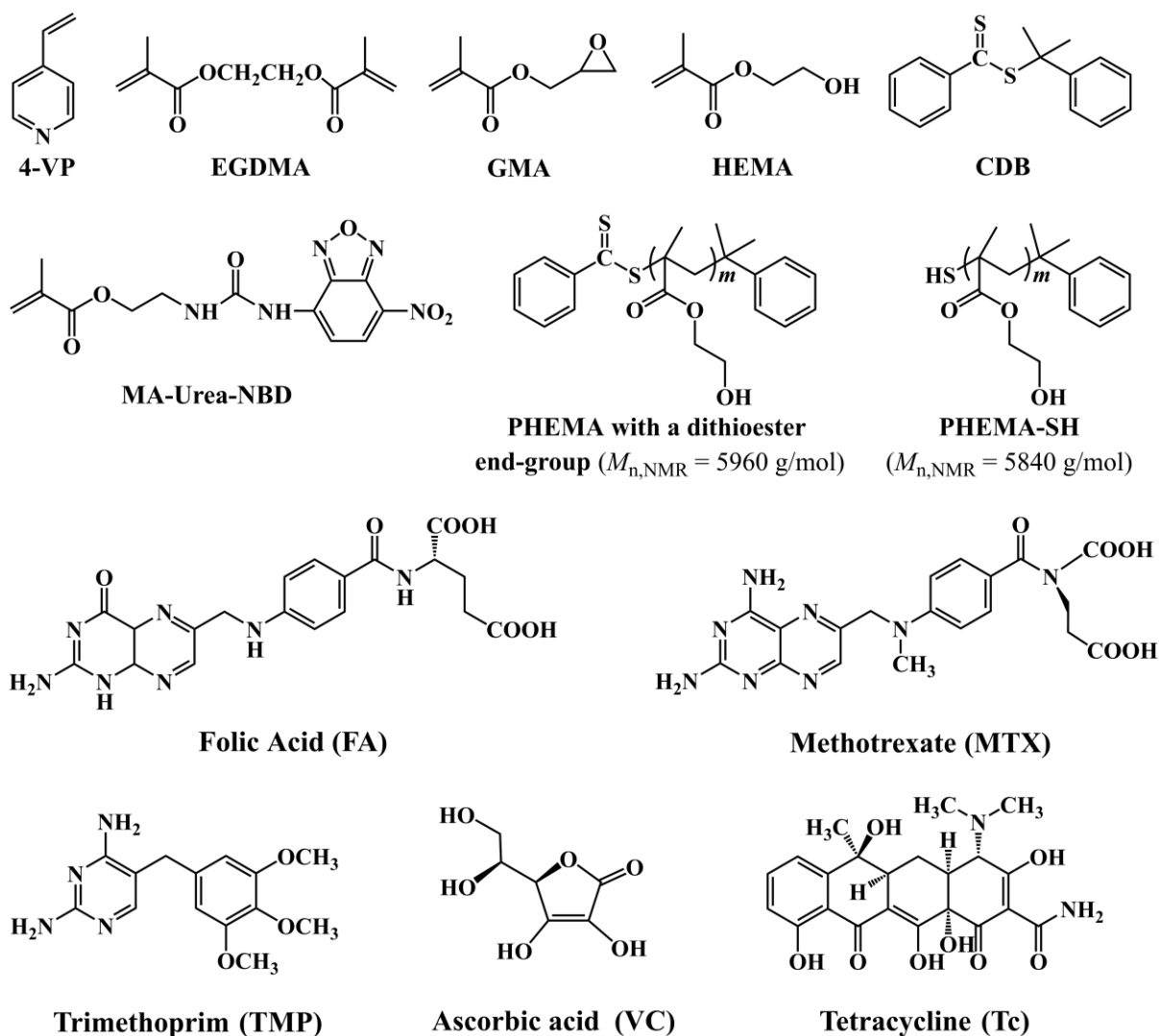
**Biological sample-compatible Au nanoparticle-containing fluorescent molecularly imprinted polymer microspheres by combining RAFT polymerization and Au-thiol chemistry**

Xiaohui Shi, Wanlan Zhang and Huiqi Zhang\*

*State Key Laboratory of Medicinal Chemical Biology, Key Laboratory of Functional Polymer Materials (Ministry of Education), Collaborative Innovation Center of Chemical Science and Engineering (Tianjin), and College of Chemistry, Nankai University, Tianjin 300071, China*

**Materials**

4-Vinylpyridine (4-VP, Alfa Aesar, 96%) was purified by distillation under vacuum. Ethylene glycol dimethacrylate (EGDMA, Alfa Aesar, 98%), glycidyl methacrylate (GMA, Shanghai Aladdin Science and Technology Co., Ltd, 97%), 2-hydroxyethyl methacrylate (HEMA, Institute of Tianjin Chemical Reagents, chemical pure), acetonitrile (Tianjin Kangkede Chemicals, Analytical grade (AR)), methanol (Tianjin Jiangtian Chemicals, AR), and azobisisobutyronitrile (AIBN, Tianjin Guangfu Fine Chemical Research Institute, AR) were purified following the literature methods.<sup>1</sup> Cumyl dithiobenzoate (CDB)<sup>2</sup> and 2-(3-(4-nitrobenzo[c][1,2,5]oxadiazol-7-yl)ureido) ethylmethacrylate (MA-Urea-NBD)<sup>3</sup> were prepared following the previously reported methods. Tetracycline (Tc) hydrochloride (Heowns Biochem Technologies, LLC, Tianjin, 97%) was converted into its neutralized form prior to use following a literature method.<sup>4</sup> Folic acid (FA, Tianjin Guangfu Fine Chemical Research Institute, 97%), methotrexate hydrate (MTX, Shanghai Leibo Chemical Technology Co., Ltd, 98%), trimethoprim (TMP, Shanghai Leibo Chemical Technology Co., Ltd, 99%), ascorbic acid (VC, Aladdin Industrial Corporation, 99%), glucose (Heowns Biochem Technologies, LLC, Tianjin, 99%), L-glutamic acid (Beijing Aoboxing Biochem Technologies, LLC, 98%), L-cysteine (Tianjin Guangfu Fine Chemical Research Institute, 99%), bovine serum album (BSA, MW = 66000, pI = 4.8, Beijing Solarbio Science & Technology Co., Ltd.), and all the other reagents were used as received. The urine samples I and II were obtained from two young male volunteers and used directly. Scheme S1 presents the chemical structures of some of the above reagents.



**Scheme S1** Chemical structures of some reagents used in the study.

### Synthesis of the “living” poly(4-VP-*co*-EGDMA) microspheres with surface-bound dithioester groups via RAFTTP

To a one-neck round-bottom flask (250 mL) with a magnetic stir bar inside were added a mixture of methanol and water (4:1 v/v, 100 mL), 4-VP (0.525 mmol), EGDMA (1.965 mmol), CDB (0.0785 mmol), and AIBN (0.0465 mmol) successively. The above mixed solution was magnetically stirred at room temperature to obtain a homogeneous solution. After being purged with argon for 30 min in an ice-water bath, the reaction mixture was sealed, magnetically stirred first at 50 °C for 2 h, and then stirred at 70 °C for 11 h (stirring rate: 150 rpm). The resulting polymer particles in the reaction solutions were collected by centrifugation, washed with methanol several times, and then dried at 40 °C under vacuum to a constant weight (yield: 48%) (entry 1 in Table 1).

## Synthesis and characterization of the thiol-terminated PHEMA (i.e., PHEMA-SH)

PHEMA-SH was prepared through first the synthesis of a PHEMA with a dithioester end-group by RAFT polymerization of HEMA and its subsequent aminolysis as shown below:

### *Synthesis of a PHEMA with a dithioester end-group*

A PHEMA with a dithioester end-group was synthesized via the RAFT polymerization of HEMA following our previously reported method as shown below:<sup>5</sup> HEMA (7.50 mmol), AIBN (15.65  $\mu$ mol), CDB (0.12 mmol), and methanol (7.5 mL) were added into a one-neck round-bottom flask (25 mL) successively. A clear purple solution was obtained after 5 min of stirring at room temperature, which was then purged with argon for 30 min in an ice-water bath, sealed, immersed into a thermostatted oil bath at 60 °C, and magnetically stirred for 48 h. The resulting reaction mixture was diluted with methanol (2.5 mL) and precipitated into ethyl ether twice to obtain a light pink polymer, which was dried at room temperature under vacuum to a constant weight to afford the product in a yield of 68 % (Table S1).

**Table S1** Synthetic condition for the PHEMA with a dithioester end-group via RAFT polymerization and its properties.

Reactant (mmol)			Solvent (mL)	Reaction temp.	Yield	$M_{n,NMR}$	$M_{n,GPC}$	$\bar{D}^b$
HEMA	CDB	AIBN	methanol	and time	(%)	(g/mol) <sup>a</sup>	(g/mol) <sup>b</sup>	
7.50	0.12	0.0157	7.5	60 °C/48 h	68%	5960	15700	1.16

<sup>a</sup> The number-average molecular weight ( $M_{n,NMR}$ ) of PHEMA with a dithioester end-group determined by <sup>1</sup>H NMR; <sup>b</sup> The number-average molecular weight ( $M_{n,GPC}$ ) and molar-mass dispersity ( $\bar{D}$ ) of the esterified form of PHEMA with a dithioester end-group determined by gel permeation chromatography (GPC) with THF as the mobile phase and polystyrene (PS) as standards (note that PHEMA with a dithioester end-group was esterified by benzoic anhydride to make it more soluble in tetrahydrofuran (THF) for GPC measurement and its esterification percentage is close to 100% as determined by <sup>1</sup>H NMR).

### *Synthesis of PHEMA-SH*

PHEMA-SH was prepared via the aminolysis of the above-obtained PHEMA with a dithioester end-group following a previously reported method.<sup>6</sup> To a one-neck round-bottom flask with a magnetic stir bar inside were added the above-obtained PHEMA with a dithioester end-group (600 mg), *n*-butylamine (0.72  $\mu$ mol), tributylphosphine (0.36 mmol), and ethanol (30 mL). After the above mixed solution was purged with argon for 20 min in an ice-water bath, the reaction system was sealed and magnetically stirred (200 rpm) at 25 °C for 3 h (the

light pink color of the polymer solution disappeared). The resulted reaction mixture was precipitated into ethyl ether twice and then dried at 40 °C under vacuum to a constant weight, leading to the white PHEMA-SH in a yield of 82% ( $M_{n,NMR} = 5840$  g/mol).

### ***Characterization of the molecular weights of PHEMA with a dithioester end-group and PHEMA-SH with $^1H$ NMR***

The number-average molecular weights of both PHEMA with a dithioester end-group and PHEMA-SH were derived from their  $^1H$  NMR spectra [Fig. S1a,b, recorded by using a Bruker Avance III 400 MHz NMR spectrometer] by using the equation:

$$M_{n,NMR} = x \times [(S_c + S_d)/S_h] \times M_{HEMA} + M_{end-groups}$$

Where  $S_c$ ,  $S_d$ , and  $S_h$  refer to the integral of the peak  $c$  around 3.90 ppm, that of the peak  $d$  around 3.60 ppm, and that of the peaks  $h$  between 7 and 8 ppm,  $M_{HEMA}$  is the molar mass of HEMA,  $M_{end-groups}$  is the total molar mass of the end-groups of the resulting polymers (e.g., for PHEMA with a dithioester end-group,  $M_{end-groups} = M_{CDB}$ ), and  $x$  is 2.5 and 1.25 for PHEMA with a dithioester end-group and PHEMA-SH, respectively.

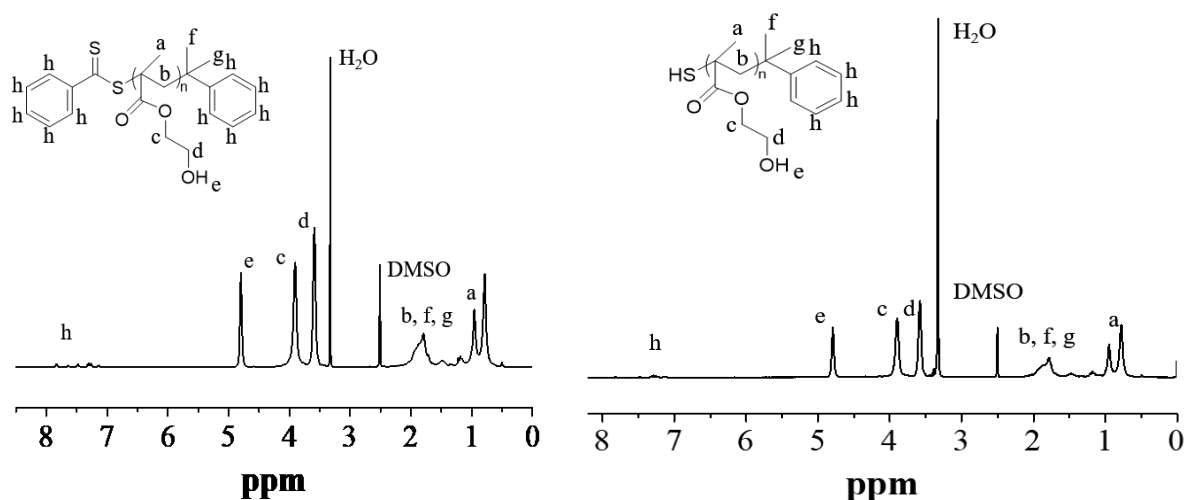


**Fig. S1**  $^1H$  NMR spectra of PHEMA with a dithioester end-group (left) and PHEMA-SH (right) in DMSO- $d_6$ .

### ***Synthesis and characterization of the esterified PHEMA macro-CTA***

The above-obtained PHEMA with a dithioester end-group was reacted with benzoic anhydride to obtain its esterified polymer (in order to make them more soluble in THF for GPC measurement) according to the following procedure:<sup>7</sup> To a one-neck round-bottom flask (10 mL) were added PHEMA with a dithioester end-group ( $M_{n,NMR} = 5960$  g/mol) (20 mg), benzoic

anhydride (2.496 mmol), dried DMF (0.6 mL), and triethylamine (2.00 mmol), successively. The mixed solution was magnetically stirred at 25 °C for 24 h. The resulting reaction mixture was precipitated into ethyl ether twice. Finally the product was dried at 40 °C under vacuum for 48 h to provide the esterified PHEMA.

The esterification percentage of the resulting polymer was close to 100%, as revealed by the complete disappearance of the peaks corresponding to the hydroxyl protons and methylene protons next to the hydroxyl groups in PGMMA macro-CTA in its  $^1\text{H}$  NMR spectrum (Fig. S2).

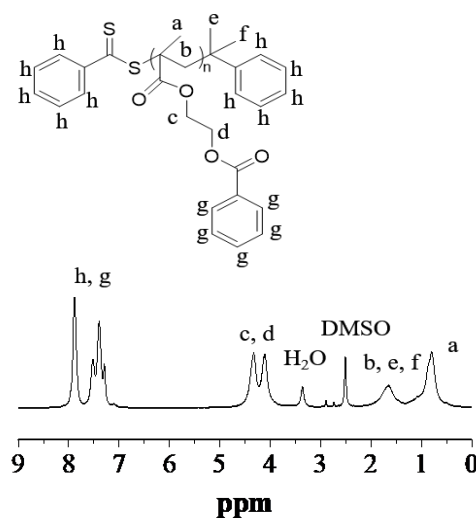


**Fig. S2**  $^1\text{H}$  NMR spectrum of the esterified PHEMA with a dithioester end-group in DMSO- $d_6$ .

GPC was used to characterize  $M_{n,\text{GPC}}$  and  $\bar{D}$  of the esterified PGMMA with a dithioester end-group, which was equipped with a Waters 717 autosampler, a Waters 1525 HPLC pump, three Waters UltraStyragel columns (with 5000-600K, 500-30K, and 100-10K molecular ranges) (the temperature of the column oven was 35 °C), and a Waters 2414 refractive index detector. THF was used as the eluent at a flow rate of 1.0 mL/min. The calibration curve was obtained by PS standards.

The  $M_{n,\text{GPC}}$  and  $\bar{D}$  of the esterified PGMMA macro-CTA were determined to be 15700 g/mol and 1.16, respectively (Table S1). Its rather small  $\bar{D}$  value indicated that the RAFT polymerization of HEMA took place in a controlled way and a well-defined PHEMA with a dithioester end-group was obtained.

### Preparation of an aqueous solution of AuNPs

An aqueous solution of AuNPs was prepared according to a literature method but with some

modification.<sup>8</sup> A solution of HAuCl<sub>4</sub> in pure water (0.01%, 300 mL) was added into a 500 mL one-neck round-bottom flask and heated to the boiling state under magnetic stirring. 7.5 mL of 1% sodium citrate solution was added quickly to the above boiling mixture. The reaction mixture was further heated in the boiling state under the magnetic stirring until the color of the solution turned to wine red. The resulting colloidal AuNP solution was then cooled down to the room temperature under stirring and was stored at 4 °C to prevent agglomeration before use. The TEM image of the resulting AuNPs is presented in Fig. 11.

### UV-vis absorption spectrum of the aqueous solution of AuNPs and fluorescence spectrum of the NBD-containing fluorescent monomer (MA-Urea-NBD) solution

A UV-vis scanning spectrophotometer (TU1900, Beijing Purkinje General Instrument Co., Ltd) was used to measure the UV-vis absorption spectrum of the sample.

All the fluorescence measurements in this work were performed on an F-4500 spectrofluorometer (Hitachi, Japan) equipped with a quartz cell (1 cm × 1 cm), the slit widths of the excitation and emission were both 10 nm, and the excitation wavelength was 420 nm with a recording emission range of 460-700 nm. The photomultiplier tube voltage was set at 650 V.

Figure S3 presents the UV-vis absorption spectrum of the aqueous solution of AuNPs and the fluorescence emission spectrum of the MA-Urea-NBD solution in methanol. The UV-vis absorption spectrum of the solution of AuNPs proved to have significant overlap with the fluorescence emission spectrum of MA-Urea-NBD, indicating that the NBD units in the MIP layer and AuNPs can function as the donor and acceptor, respectively. Therefore, there should exist fluorescence resonance energy transfer (FRET) between the NBD units in the MIP layer

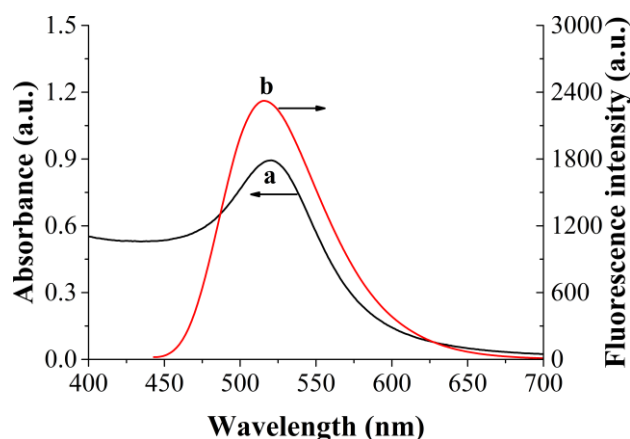


**Fig. S3** (a) UV-vis absorption spectrum of the aqueous solution of AuNPs. (b) Fluorescence spectrum of MA-Urea-NBD solution in methanol (0.54 mM).

and AuNPs directly attached on the MIP layer surface because their distance is within 10 nm.<sup>9</sup> When an lcPGMA layer with a thickness of 28 nm was introduced between the fluorescent MIP layer and AuNPs, the FRET between the NBD units in the MIP layer and AuNPs became negligible because of their too large distance.<sup>9</sup>

### **Characterization of the morphologies, particle sizes, and size distribution indices of the polymer particles with SEM**

The morphologies of the polymer particles were characterized with a scanning electron microscope (SEM, JSM-7500F) (Fig. 1a-k). The SEM size data of the polymer particles reflect the averages of about 200 particles, which are calculated by the following formulas (Table 1):<sup>10</sup>

$$D_n = \sum_{i=1}^k n_i D_i / \sum_{i=1}^k n_i; \quad D_w = \sum_{i=1}^k n_i D_i^4 / \sum_{i=1}^k n_i D_i^3; \quad U = D_w / D_n$$

where  $D_n$  is the number-average diameter,  $D_w$  the weight-average diameter,  $k$  the total number of the measured particles,  $D_i$  the particle diameter of the  $i$ th polymer microsphere,  $n_i$  the number of the microspheres with a diameter  $D_i$ , and  $U$  the size distribution index.

### **Transmission electron microscope (TEM) analyses**

The samples were characterized with a field emission TEM (Talos L120C G2) (Fig. 1l-n). The TEM samples were prepared by dropping a drop of each aqueous dispersed sample onto the surface of a copper grid coated with a carbon membrane and then dried under vacuum at room temperature prior to the measurement.

### **FT-IR characterization of the polymer particles**

The Fourier-transform infrared (FT-IR) spectra of the samples were obtained using a TENSOR II (Bruker) FT-IR spectrometer.

### **Dispersion stability of the polymer particles in pure water**

The dispersion stability of poly(4-VP-co-EGDMA) particles and all the obtained fluorescent MIP/CP particles (entries 1-11 in Table 1) in pure water was studied. After their ultrasonic dispersion in pure water (1.0 mg/mL), the dispersed mixtures were allowed to settle down for 0 h (Fig. 3a) and 3 h (Fig. 3b) at 25 °C.

### **Equilibrium template binding experiments with FA-MIPs/FA-CPs in different media**

Equilibrium binding experiments were performed by incubating a FA solution (0.5 mL,  $C = 0.02$  mM) in ACN/DMF (4:1 v/v) or the undiluted urine sample I with different amounts of MIPs/CPs at 25 °C for 8 h in the dark. After centrifugation, the amounts of FA remaining in the supernatants ( $F$ ) were quantified by using HPLC (Scientific System Inc., USA) equipped with an UV-vis detector and a Lanbo Kromasil C18 column (250 mm  $\times$  4.6 mm), from which the amounts of FA bound to the MIPs/CPs [i.e., Bound (%)] could be obtained [Bound (%) =  $[(C_0 - F)/C_0] \times 100\%$ , where  $C_0$  is the initial FA concentration in the studied solution, and  $F$  the FA concentration in the solution after the equilibrium binding is reached]. The wavelength used for the determination of FA was 288 nm. A mixture of methanol/ACN (1:1 v/v) and aqueous solution of trifluoroacetic acid (pH = 2) (30:70 v/v) was used as the mobile phase at a flow rate of 0.8 mL/min. All the above binding analyses were performed in duplicate and the mean values were used.

### ***Equilibrium template binding experiments with FA-MIPs/FA-CPs in the organic solvent***

The equilibrium template bindings of the studied MIPs/CPs (including polym@NBD-MIP/CP, polym@NBD-MIP/CP@lcPGMA, polym@NBD-MIP/CP@lcPGMA-SH, polym@NBD-MIP/CP@lcPGMA@AuNPs, and polym@NBD-MIP/CP@lcPGMA@AuNPs@PHEMA) in the organic solvent [i.e., ACN/DMF (4:1 v/v)] were first studied. It can be seen clearly from Fig. S4a-e that all the studied FA-MIPs could bind more of the template than their corresponding FA-CPs in the organic solvent, suggesting their presence of imprinted binding sites. In particular, it is worth noting that although the binding capacities of these MIPs/CPs are somewhat different because of their different surface or matrix properties [leading to their different nonspecific bindings (which can be represented by the bindings of the CPs)], their specific bindings (i.e., the binding differences between MIPs and their CPs) are almost the same. These results indicated that the surface-modification of MIPs/CPs had negligible influence on the imprinted binding sites.

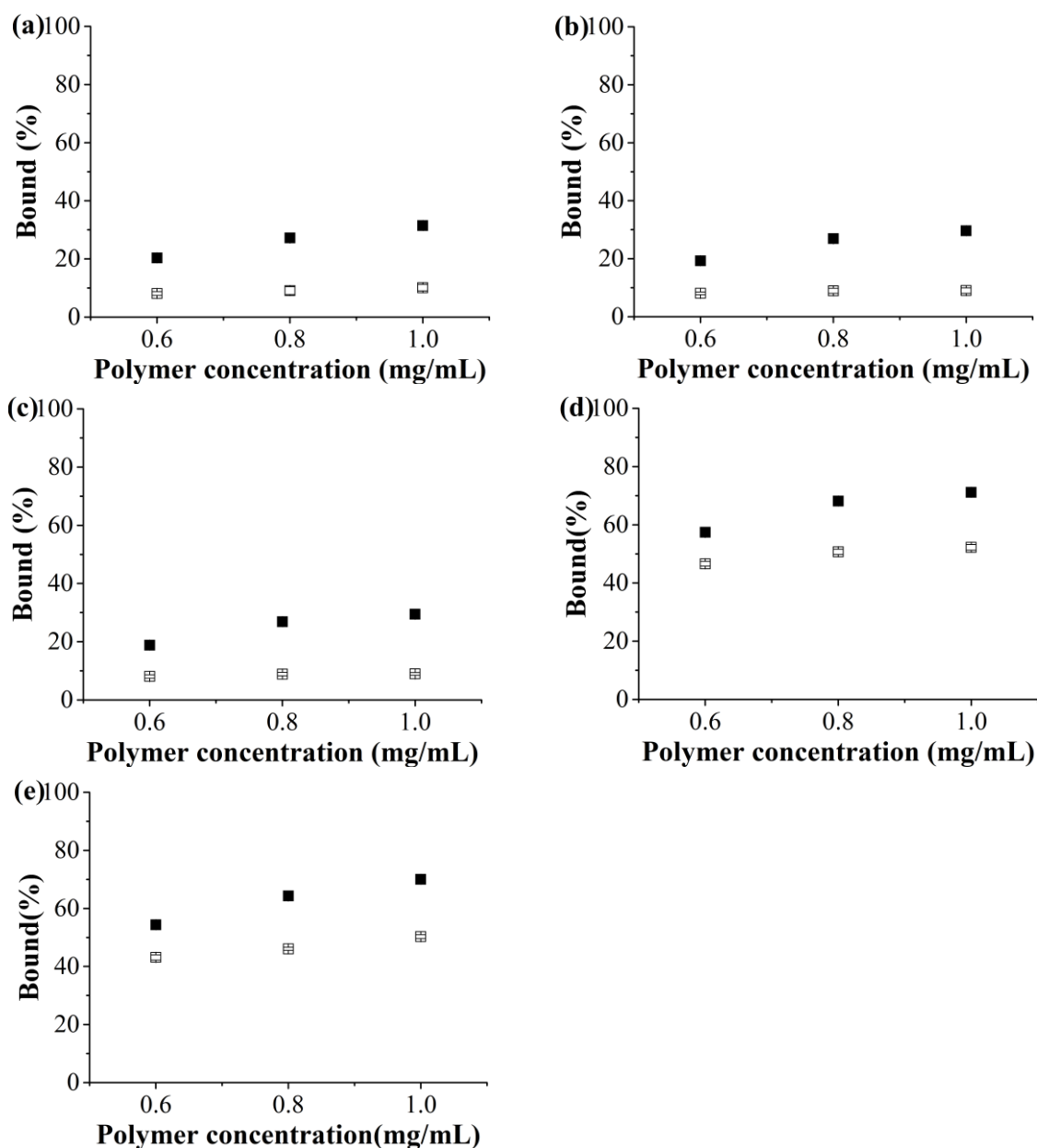


**Fig. S4** Equilibrium template bindings of MIPs (filled symbols)/CPs (open symbols) [including polym@NBD-MIP/CP (a), polym@NBD-MIP/CP@lcPGMA (b), polym@NBD-MIP/CP@lcPGMA-SH (c), polym@NBD-MIP/CP@lcPGMA@AuNPs (d), and polym@NBD-MIP/CP@lcPGMA@AuNPs@PHEMA (e)] in FA solution (0.02 mM) in ACN/DMF (4:1 v/v) at 25 °C.

#### ***Equilibrium template binding experiments with FA-MIPs/FA-CPs in the undiluted urine***

The equilibrium binding properties of the ungrafted and grafted AuNP-containing fluorescent MIPs/CPs (entries 8-11, Table 1) were then studied in the undiluted urine sample I. As expected, the specific bindings of the ungrafted MIP (entry 8, Table 1) disappeared (Fig. S5a),

mainly due to its high surface hydrophobicity.<sup>10</sup> In sharp contrast, the specific bindings of the grafted MIP (entry 10, Table 1) in urine sample I are almost the same as those in the organic solvent (Fig. S5b), demonstrating their high compatibility with the complex biological sample. Note that the binding capacities of the grafted AuNP-containing fluorescent MIP and CP particles in the undiluted urine samples are higher than their binding capacities found in the organic solvent (Fig. S5b), which could be attributed to their still not high enough surface hydrophilicity (thus leading to relatively higher nonspecific bindings).<sup>7</sup>

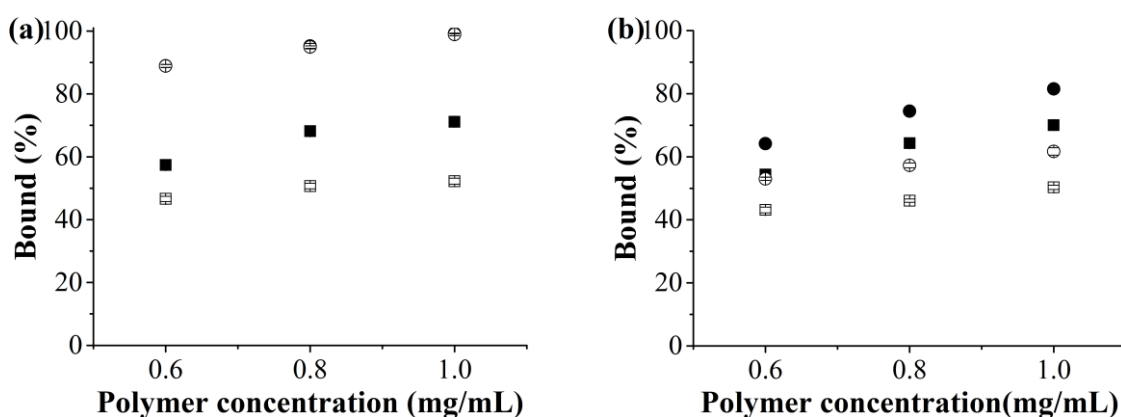


**Fig. S5** Equilibrium template bindings of MIPs (filled symbols)/CPs (open symbols) [including polym@NBD-MIP/CP@lcPGMA@AuNPs (a) and polym@NBD-MIP/CP@lcPGMA@AuNPs@PHEMA (b)] in FA solution (0.02 mM) in ACN/DMF (4:1 v/v) (squares) or the undiluted pure urine sample I (circles) at 25 °C.

### Competitive binding experiments with the ungrafted and grafted AuNP-containing fluorescent FA-MIPs/FA-CPs in the organic solvent and the undiluted urine, respectively

Competitive binding experiments of the ungrafted and grafted AuNP-containing fluorescent FA-MIPs/FA-CPs were evaluated by measuring their competitive bindings towards FA and its structurally related compounds MTX and TMP (Scheme S1) in ACN/DMF (4:1 v/v) or in the undiluted urine sample I as follows: 0.5 mg of the ungrafted or grafted FA-MIP/FA-CP were incubated with 0.5 mL of a mixed solution of FA, MTX, and TMP ( $C_{\text{FA}}$  or  $C_{\text{MTX}}$  or  $C_{\text{TMP}} = 0.02$  mM) in ACN/DMF (4:1 v/v) or in the undiluted urine sample I at 25 °C for 8 h. After centrifugation, the amounts of the analytes remaining in the supernatants ( $F$ ) were determined by HPLC, from which the amounts of the analytes bound to the MIPs/CPs [i.e.,  $B = (C_0 - F)V/m$ , where  $C_0$  is the initial analyte concentration in the studied solution,  $F$  the analyte concentration in the

solution after the equilibrium binding is reached,  $V$  the volume of the studied solution, and  $m$  the mass of the MIP or CP] could be derived. The wavelength used for the determination of FA, MTX or TMP was 288 nm. A mixture of methanol/ACN (1:1 v/v) and aqueous solution of trifluoroacetic acid (pH = 2) (30:70 v/v) was used as the mobile phase at a flow rate of 0.8 mL/min. All the binding analyses were performed in duplicate and the mean values were used.

Fig. S6a,b presents the selective (or competitive) bindings of the ungrafted and grafted FA-MIPs/FA-CPs toward FA, MTX, and TMP in their mixed solution in the organic solvent and pure urine sample I, respectively.

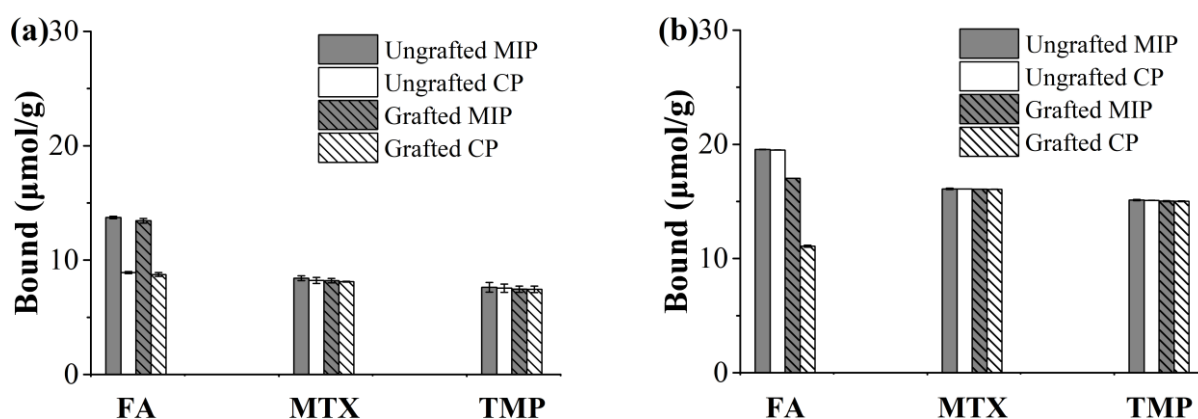


**Fig. S6** Selective bindings of the ungrafted and grafted AuNP-containing fluorescent MIPs/CPs toward FA, MTX, and TMP in their mixed solutions ( $C_{FA}$  or  $MTX$  or  $TMP$  = 0.02 mM) in ACN/DMF (4:1 v/v) (a) or the undiluted pure urine sample I (b) at 25 °C (polymer concentration: 1 mg/mL).

To quantitatively characterize the binding selectivity of the ungrafted and grafted FA-MIPs/FA-CPs, the “imprinting-induced promotion of binding” (IPB) was applied in this study. IPB has proven to be a useful parameter for evaluating the MIPs’ selectivity because the difference in the intrinsic nonspecific bindings of the MIPs towards different analytes is normalized.<sup>11</sup> IPB can be defined by the following equation:

$$IPB (\%) = [(B_{MIP} - B_{CP})/B_{CP}] \times 100\%$$

where  $B_{MIP}$  and  $B_{CP}$  are equilibrium bindings of the MIP and its CP toward an analyte, respectively. The larger the IPB of the MIP toward the analyte, the better its selectivity.

The IPB values determined for both the ungrafted and grafted FA-MIPs in both ACN/DMF (4:1 v/v) and the undiluted pure urine I are listed in Table S2, which demonstrated clearly that the grafted FA-MIP showed obvious selectivity toward FA in both the organic solvent and in

pure urine, whereas no selectivity toward FA was observed for the ungrafted FA-MIP in pure urine although it showed good selectivity toward FA in the organic solvent.

**Table S2.** Selective binding properties of the ungrafted and grafted AuNP-containing fluorescent FA-MIPs/FA-CPs toward FA, MTX, and TMP in different media.

Solvent	Analyte	The ungrafted FA-MIP/FA-CP			The grafted FA-MIP/FA-CP		
		$B_{\text{MIP}}^a$	$B_{\text{CP}}^a$	IPB (%) <sup>b</sup>	$B_{\text{MIP}}^a$	$B_{\text{CP}}^a$	IPB (%) <sup>b</sup>
ACN/ DMF (4:1 v/v)	FA	13.74 ± 0.11	8.91 ± 0.09	54	13.45 ± 0.20	8.74 ± 0.17	54
	MTX	8.42 ± 0.21	8.22 ± 0.27	2	8.21 ± 0.19	8.12 ± 0.04	1
	TMP	7.62 ± 0.42	7.55 ± 0.36	1	7.46 ± 0.27	7.45 ± 0.28	0
Pure Urine sample I	FA	19.55 ± 0.02	19.51 ± 0.04	0	17.04 ± 0.01	11.07 ± 0.09	54
	MTX	16.10 ± 0.06	16.09 ± 0.01	0	16.08 ± 0.02	16.07 ± 0.01	0
	TMP	15.13 ± 0.05	15.09 ± 0.04	0	15.03 ± 0.07	15.02 ± 0.04	0

<sup>a</sup>  $B_{\text{MIP}}$  and  $B_{\text{CP}}$  are equilibrium binding capacities of the MIP and its corresponding CP toward FA, MTX and TMP in their mixed solution ( $C_{\text{FA or TMP or MTX}} = 0.02 \text{ mM}$ ) in different media, which are the same as those shown in Fig. S6 and have a unit of  $\mu\text{mol/g}$ ; <sup>b</sup> IPB refers to the “imprinting-induced promotion of binding” value of the studied MIP.

**Optosensing properties of the grafted AuNP-containing fluorescent FA-MIP/FA-CP (i.e., polym@NBD-MIP/CP@lcPGMA@AuNPs@PHEMA) in the undiluted urine samples**

***Photostability measurements of the grafted AuNP-containing fluorescent FA-MIP/FA-CP***

The photostability of grafted AuNP-containing fluorescent FA-MIP/FA-CP was determined by measuring the changes in the fluorescence intensities of their aqueous solutions ( $0.25 \text{ mg mL}^{-1}$ ) over time at 25 °C under air atmosphere (Fig. 4a).

***Reusability tests of the grafted AuNP-containing fluorescent FA-MIP/FA-CP***

The reusability of the grafted AuNP-containing fluorescent FA-MIP/FA-CP was assessed by measuring the changes in the fluorescence intensities of their pure urine sample I solutions ( $1.0 \text{ mg/mL}$ ) after their consecutive FA adsorption-desorption cycles as follows:  $0.25 \text{ mg}$  of the grafted AuNP-containing fluorescent FA-MIP or FA-CP was first dispersed in  $1.0 \text{ mL}$  of the undiluted pure urine sample I, and the fluorescence intensity of the mixed solution was determined. After centrifugation of the above mixture and removal of the supernatant, the resulting MIP or CP was mixed with  $1.0 \text{ mL}$  of FA solution ( $15 \mu\text{M}$ ) in pure urine sample I and then incubated at 25 °C for 2 h. The fluorescence intensity of the above mixture was then

determined. Afterwards, the above mixture was centrifuged again. The resulting MIP or CP with bound FA was washed with water and methanol successively (until no FA was detectable in the washing solutions). After centrifugation and removal of the supernatant, the resulting MIP or CP was further mixed with 1.0 mL of pure urine sample I and the fluorescence intensity of the above mixture was again determined. The above procedure was repeated for 10 cycles and the results are presented in Fig. 4b.

### ***Binding kinetics of the grafted AuNP-containing fluorescent FA-MIP/FA-CP in the undiluted urine***

The time responses (or binding kinetics) of the grafted AuNP-containing fluorescent FA-MIP/FA-CP were studied by incubating a certain amount of MIP/CP ( $0.25 \text{ mg mL}^{-1}$ ) with a FA solution in the undiluted urine sample I ( $15 \text{ }\mu\text{M}$ ) for different times and their fluorescence spectra were recorded for analyses.

Figs. 5a and S7 present the fluorescence spectra of the grafted AuNP-containing fluorescent FA-MIP and FA-CP after their incubation with a FA solution ( $15 \text{ }\mu\text{M}$ ) at  $25 \text{ }^{\circ}\text{C}$  for different times in pure urine sample I, respectively, from which their binding kinetics could be derived (Fig. 5b).

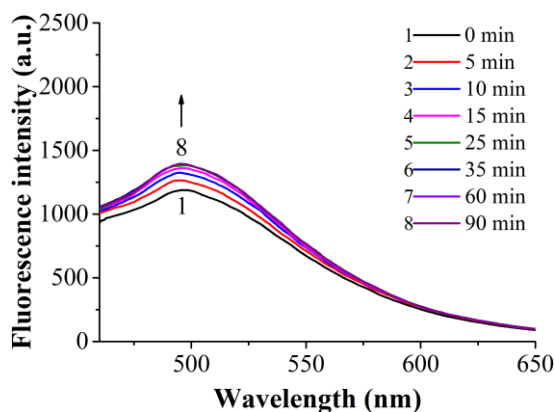


**Fig. S7** Fluorescence spectra of the grafted AuNP-containing fluorescent FA-CP ( $0.25 \text{ mg/mL}$ ) after its incubation with a FA solution ( $15 \text{ }\mu\text{M}$ ) in the undiluted pure urine sample I at  $25 \text{ }^{\circ}\text{C}$  for different times.

### ***Fluorescence titration experiments of the grafted AuNP-containing fluorescent FA-MIP/FA-CP in the undiluted urine samples***

The optosensing properties of the grafted AuNP-containing FA-MIP/FA-CP were studied by analyzing the fluorescence enhancement upon their binding with FA in the undiluted urine as

follows: 0.25 mg of the grafted AuNP-containing fluorescent FA-MIP/FA-CP were incubated with a solution of FA (0, 5, 10, 15, 20, 30, 40, or 50  $\mu$ M, 1.0 mL) in pure urine sample I at 25 °C for 2 h, and their fluorescence spectra were recorded for analyses (Fig. 6a,b).

The fluorescence enhancement efficiency of the grafted AuNP-containing fluorescent FA-MIP/FA-CP was calculated by using the Stern-Volmer equation as shown below:

$$F/F_0 = 1 + K_{SV}C$$

where  $F_0$  and  $F$  are the fluorescence intensities in the absence and presence of FA, respectively,  $K_{SV}$  the Stern-Volmer constant, and  $C$  the FA concentration.

Fig. 6c presents the fluorescence enhancement efficiency of studied FA-MIP/FA-CP by FA, which clearly demonstrated that the grafted AuNP-containing fluorescent FA-MIP could be enhanced by FA more efficiently than its CP.

#### ***Optosensing selectivity of the grafted AuNP-containing fluorescent FA-MIP/FA-CP in the undiluted urine samples***

The optosensing selectivity of the grafted AuNP-containing fluorescent FA-MIP/FA-CP in pure urine sample I was evaluated through comparing their fluorescence enhancement by FA and its structurally related compounds MTX and TMP as well as some other drugs (i.e., VC and Tc) (Scheme S1) as follows: 0.25 mg of the grafted FA-MIP/FA-CP were incubated with a solution of FA, MTX, TMP, VC or Tc in urine sample I (15  $\mu$ M, 1.0 mL) at 25 °C for 2 h, and their fluorescence spectra were recorded for analyses (Fig. 7a).

The optosensing selectivity of the grafted FA-MIP/FA-CP in pure urine sample I was also evaluated through comparing their fluorescence enhancement by FA and some other compounds such as glucose, L-cysteine, L-glutamic acid, and BSA as follows: 0.25 mg of the grafted FA-MIP/FA-CP were incubated with a solution of glucose, L-cysteine, L-glutamic acid, or BSA in urine I (15  $\mu$ M, 1.0 mL) at 25 °C for 2 h, and their fluorescence spectra were recorded for analyses (Fig. 7b).

The optosensing selectivity of the grafted FA-MIP/FA-CP in pure urine sample I was further evaluated by testing their fluorescence responses to FA (15  $\mu$ M) in the presence of 10-fold of one of the above-mentioned compounds (i.e., MTX, TMP, VC, Tc, glucose, L-cysteine, L-glutamic acid, or BSA) as follows: 0.25 mg of the grafted FA-MIP/FA-CP were incubated with a solution of FA (15  $\mu$ M, 1.0 mL) in urine I in the presence of 10-fold of MTX, TMP, VC,

Tc, glucose, L-cysteine, L-glutamic acid, or BSA at 25 °C for 2 h, and their fluorescence spectra were recorded for analyses (Fig. 7c,d).

***Direct quantification of FA with the grafted AuNP-containing fluorescent FA-MIP in the undiluted urine samples***

Direct fluorescent quantification of FA with the grafted AuNP-containing fluorescent FA-MIP/FA-CP in the undiluted urine sample II was performed as follows (Table 2):

- 1) 0.25 mg of the studied FA-MIP was incubated with 1.0 mL of FA solution in the undiluted urine sample II (0, 0.5, 5 or 10  $\mu$ M) at 25 °C for 2 h, and their fluorescence spectra were recorded for analyses.
- 2) 0.25 mg of the studied FA-MIP was incubated with 1.0 mL of a mixed solution of FA (0, 0.5, 5 or 10  $\mu$ M) and some other compounds including TMP, VC, and Tc (their concentrations are the same as FA in each solution) in urine sample II at 25 °C for 2 h, and their fluorescence spectra were recorded for analyses.

**Effect of the incorporated AuNPs on the optosensing sensitivity of the fluorescent MIPs/CPs**

***Fluorescence titration experiments of polym@NBD-MIP/CP and polym@NBD-MIP/CP@lcPGMA@AuNPs in the organic solvent***

The optosensing properties of polym@NBD-MIP/CP and polym@NBD-MIP/CP@lcPGMA@AuNPs were studied by analyzing the fluorescence enhancement upon their binding with FA in ACN/DMF (4:1 v/v) as follows: 0.25 mg of the studied FA-MIP/FA-CP were incubated with a solution of FA (0, 5, 10, 15, 30, or 50  $\mu$ M, 1.0 mL) in ACN/DMF (4:1 v/v) at 25 °C for 2 h, and their fluorescence spectra were recorded for analyses (Fig. 8a,c and Fig. S8a,b).

Fig. 8b,d presents the fluorescence enhancement efficiency of the studied FA-MIPs/FA-CPs, which was calculated by using the Stern-Volmer equation as described in the manuscript on the basis of results shown in Fig. 8a,c and Fig. S8a,b.

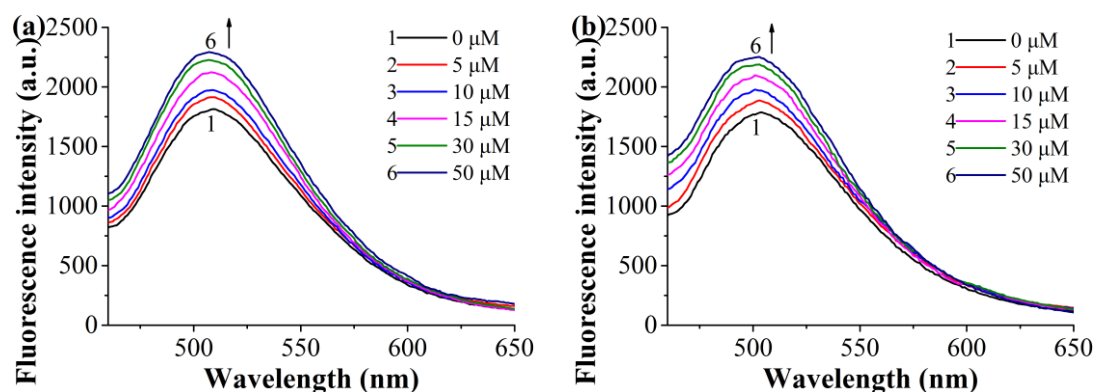


**Fig. S8** Fluorescence spectra of polym@NBD-CP (a) and polym@NBD-CP@lcPGMA@AuNPs (b) (0.25 mg/mL) upon their exposure to different concentrations of FA in ACN/DMF (4:1 v/v) at 25 °C.

## References

- 1) Y. Ma, J. Gao, C. Zheng and H. Zhang, *J. Mater. Chem. B*, 2019, **7**, 2474-2483.
- 2) T. P. Le, G. Moad, E. Rizzardo and S. H. Thang, *U.S. Patent 7,666,962 B2*, 2010.
- 3) W. Wan, M. Biyikal, R. Wagner, B. Sellergren and K. Rurack, *Angew. Chem., Int. Ed.*, 2013, **52**, 7023-7027.
- 4) L. Schweitz, P. Spégel and S. Nilsson, *Analyst*, 2000, **125**, 1899-1901.
- 5) Y. Ma, G. Pan, Y. Zhang, X. Guo and H. Zhang, *Angew. Chem., Int. Ed.*, 2013, **52**, 1511-1514.
- 6) M. Li, P. De, S. R. Gondi and B. S. Sumerlin, *J. Polym. Sci., Part A: Polym. Chem.*, 2008, **46**, 5093-5100.
- 7) M. Zhao, C. Zhang, Y. Zhang, X. Guo, H. Yan and H. Zhang, *Chem. Commun.*, 2014, **50**, 2208-2210.
- 8) J. Fei, W. Dou and G. Zhao, *RSC Adv.*, 2015, **5**, 74548-74556.
- 9) S. Y. Lim, J. H. Kim, J. S. Lee, J. Ahn, M.-G. Kim and C. B. Park, *J. Mater. Chem.*, 2011, **21**, 17623-17626.
- 10) M. Zhao, X. Chen, H. T. Zhang, H. Yan and H. Zhang, *Biomacromolecules*, 2014, **15**, 1663-1675.
- 11) T. Hishiya, M. Shibata, M. Kakazu, H. Asanuma and M. Komiyama, *Macromolecules*, 1999, **32**, 2265-2269.